

Phosphoinositide Binding Differentially Regulates NHE1 Na⁺/H⁺ Exchanger-dependent Proximal Tubule Cell Survival^{*[5]}

Received for publication, December 15, 2010, and in revised form, October 18, 2011. Published, JBC Papers in Press, October 21, 2011, DOI 10.1074/jbc.M110.212845

Bassam G. Abu Jawdeh[‡], Shenaz Khan[‡], Isabelle Deschênes^{‡§}, Malcolm Hoshi[§], Monu Goel[§], Jeffrey T. Lock[§], Krekwit Shinlapawittayatorn[§], Gerald Babcock^{‡§}, Sujata Lakhe-Reddy[‡], Garren DeCaro[‡], Satya P. Yadav[¶], Maradumane L. Mohan[¶], Sathyamangla V. Naga Prasad[¶], William P. Schilling^{‡§}, Eckhard Ficker[‡], and Jeffrey R. Schelling^{‡¶1}

From the Departments of [‡]Medicine, [§]Physiology and Biophysics, Lerner Research Institute, [¶]Cleveland Clinic Foundation, Case Western Reserve University, Cleveland, Ohio 44109

Background: Chronic kidney disease is perpetuated by tubular epithelial cell apoptosis, and the NHE1 Na⁺/H⁺ exchanger defends against apoptosis in response to undefined regulatory mechanisms.

Results: Phosphatidylinositol 4,5-bisphosphate (PI(4,5)P₂) and phosphatidylinositol 3,4,5-trisphosphate (PI(3,4,5)P₃) bind and differentially regulate NHE1 through weak electrostatic and pH-dependent interactions.

Conclusion: NHE1-phospholipid binding regulates NHE1 activities.

Significance: NHE1-dependent cell survival is mediated through toggling between interactions with PI(4,5)P₂ and PI(3,4,5)P₃.

Tubular atrophy predicts chronic kidney disease progression, and is caused by proximal tubular epithelial cell (PTC) apoptosis. The normally quiescent Na⁺/H⁺ exchanger-1 (NHE1) defends against PTC apoptosis, and is regulated by PI(4,5)P₂ binding. Because of the vast array of plasma membrane lipids, we hypothesized that NHE1-mediated cell survival is dynamically regulated by multiple anionic inner leaflet phospholipids. In membrane overlay and surface plasmon resonance assays, the NHE1 C terminus bound phospholipids with low affinity and according to valence (PIP₃ > PIP₂ > PIP = PA > PS). NHE1-phosphoinositide binding was enhanced by acidic pH, and abolished by NHE1 Arg/Lys to Ala mutations within two juxtamembrane domains, consistent with electrostatic interactions. PI(4,5)P₂-incorporated vesicles were distributed to apical and lateral PTC domains, increased NHE1-regulated Na⁺/H⁺ exchange, and blunted apoptosis, whereas NHE1 activity was decreased in cells enriched with PI(3,4,5)P₃, which localized to basolateral membranes. Divergent PI(4,5)P₂ and PI(3,4,5)P₃ effects on NHE1-dependent Na⁺/H⁺ exchange and apoptosis were confirmed by selective phosphoinositide sequestration with pleckstrin homology domain-containing phospholipase Cδ and Akt peptides, PI 3-kinase, and Akt inhibition in wild-type and NHE1-null PTCs. The results reveal an on-off switch model, whereby NHE1 toggles between weak interactions with PI(4,5)P₂ and PI(3,4,5)P₃. In response to apoptotic stress, NHE1 is stimulated by PI(4,5)P₂, which leads to PI 3-kinase activation, and PI(4,5)P₂ phosphorylation. The resulting PI(3,4,5)P₃ dually stimulates sustained, downstream Akt survival signaling, and dampens NHE1 activity through competitive inhibition and depletion of PI(4,5)P₂.

Chronic kidney diseases affect more than 26 million people in the United States (1), and over 500,000 people require renal replacement therapy, at an annual Medicare cost of \$24 billion (2). Tubular atrophy is a hallmark of chronic kidney disease progression, and is superior to glomerular histopathology as a predictor of clinical outcomes (3–6). Proximal renal tubular epithelial cell (PTC)² apoptosis is a prominent feature in human renal biopsies and mouse models of chronic, progressive kidney diseases, and an important mechanism of tubular atrophy (7–12).

Apoptosis is characterized by cell volume shrinkage and cytosol acidification (13), which favor activation of pro-apoptotic caspases (14, 15), Bax (16), and Smac/DIABLO (17), consistent with a pH threshold for triggering cell death pathways. The NHE1 Na⁺/H⁺ exchanger is expressed on the basolateral plasma membrane of epithelial cells (18), and is normally quiescent (19, 20). NHE1 counteracts apoptosis in the proximal tubule and other tissues (21), in part through Na⁺ influx and H⁺ extrusion, resulting in restoration of cell volume and cytosolic pH, respectively. In addition, the NHE1 C-terminal tail serves as a scaffold for assembly of signaling modules (22, 23). Multiple NHE1 stimuli have been identified, including growth factors, integrins, hypertonicity, and apoptotic stress, but the mechanisms regulating NHE1 activation and inactivation in response to apoptotic stress have not been described.

The plasma membrane inner leaflet phospholipid PI(4,5)P₂ binds to and regulates multiple ion channels and exchangers (24–28), including NHE1 (29–31), consistent with studies suggesting that in some cell types NHE1 is compartmentalized to lipid rafts (30, 32, 33), which may be enriched for phosphoi-

* This work was supported, in whole or in part, by National Institutes of Health Grants R01 DK067528 and R01 DK072348 (to J. R. S.) and R01 HL097355 (to W. P. S.) and an American Heart Association fellowship grant (to B. G. A. J.).

[5] The on-line version of this article (available at <http://www.jbc.org>) contains supplemental Figs. S1–S5.

¹ To whom correspondence should be addressed: Rammelkamp Center for Research, 2500 MetroHealth Dr., R415, Cleveland, OH 44109. Tel.: 216-778-4993; Fax: 216-778-4321; E-mail: jeffrey.schelling@case.edu.

² The abbreviations used are: PTC, proximal renal tubular epithelial cell; cNHE1, NHE1 cytosolic domain; TIRF, total internal reflection fluorescence; EIPA, N-ethyl-N-isopropyl amiloride; PC, phosphatidylcholine; PI, phosphatidylinositol; PA, phosphatidic acid; PS, phosphatidylserine; LPA, lysophosphatidic acid; PE, phosphatidylethanolamine; PLC, phospholipase C; PH, pleckstrin homology; BCECF, 2',7'-bis(2-carboxyethyl)-5,6-carboxyfluorescein; ZO-1, zona occludens-1; LPC, lysophosphatidylcholine; S-1p, sphingosine 1-phosphate.

Phosphoinositides Regulate NHE1

nositides (34). PI(4,5)P₂ is the most abundant phosphoinositide, comprising ~1% of the plasma membrane phospholipid content (35). The estimated PI(4,5)P₂ concentration is 10–15 μM, although localized concentrations within membrane microdomains may be higher (36–38). PI(4,5)P₂ has pleiotropic functions, most notably as a substrate for hydrolysis by phospholipase C, and phosphorylation by PI 3-kinase to form PI(3,4,5)P₃, which docks amphipathic Akt, leading to its activation and phosphorylation of downstream targets that mediate cell survival. PI(4,5)P₂ has been associated with enhanced NHE1-dependent Na⁺/H⁺ exchange (29, 30), as well as inhibition of apoptosis through inactivation of caspases (39), suggesting a convergent mechanism of cytoprotection through PI(4,5)P₂-NHE1 interaction.

Regulation of NHE1 is complex, involving multiple protein binding partners. Because NHE1 is a transmembrane protein there is also potential for association and regulation by membrane lipids. However, interaction between PI(4,5)P₂ and the NHE1 cytosolic tail is the sole example of a phospholipid binding with the exchanger. Other plausible candidates include PI(3,4,5)P₃, which carries a relatively greater negative charge (–6 versus –4 for PI(4,5)P₂), and phosphatidylserine (PS), which is more abundant than PI(4,5)P₂, and perpetuates apoptosis by translocating from the inner to outer plasma membrane leaflet (40). In this report, we show that NHE1 is regulated by toggling between low affinity interactions with PI(4,5)P₂ and PI(3,4,5)P₃.

EXPERIMENTAL PROCEDURES

Materials—His₆ peptide (Covance, Princeton, NJ), LY-294002 (Calbiochem, San Diego, CA), staurosporine, wortmannin, cisplatin (Sigma), and Akt VIII (Chemdea, Ridgewood, NJ) were used. M1, M2, and M1 + M2 mutant rat NHE1 cDNAs were gifts from Dr. John Orlowski (McGill University). NHE1 rabbit polyclonal antibody was a gift from Dr. Josette Noel (University of Montreal)(41). GFP-tagged PLCδ-PH and Akt-PH plasmids were gifts from Dr. Tamas Balla (National Institutes of Health, NICHD). Purchased antibodies included mouse monoclonal anti-poly-His (Alpha Diagnostic, San Antonio, TX), rat monoclonal anti-zona occludens-1 (ZO-1; Chemicon, Temecula, CA), rabbit polyclonal anti-active caspase-3 (Cell Applications, San Diego, CA), rabbit monoclonal anti-GAPDH (Cell Signaling, Danvers, MA), Texas Red-conjugated goat anti-rabbit IgG and AF488-conjugated goat anti-rat IgG (Invitrogen) and peroxidase-conjugated donkey anti-rabbit IgG (Amersham Biosciences).

Cell Culture—LLC-PK1 cells were purchased from ATCC (Manassas, VA) and maintained in DMEM (Invitrogen) plus 10% fetal bovine serum (HyClone, Logan, UT). C57BL/6 wild-type and NHE1-null C57BL/6^{Swe/Swe} (42) proximal tubule cells were derived from mice, which were purchased from Jackson Laboratories. Proximal tubules were isolated by Percoll gradient centrifugation (43), maintained in primary culture in DMEM/F-12 (Invitrogen) plus 10% fetal bovine serum (HyClone), and then immortalized by infection with temperature-sensitive SV40. Cell lines were propagated at 33 °C, and then studied under differentiating conditions after 24 h at 37 °C. In some experiments, cells were cultured on permeable

supports (Costar Corning, Lowell, MA) to generate polarized monolayers. For experiments to assess NHE1 and phosphoinositide membrane domain sorting, we used 24-mm diameter, 0.4-μm pore, polyester membrane supports (Costar number 3450). For experiments to assess single cell NHE1 Na⁺/H⁺ exchange activity, 12-mm 0.4-μm pore supports (Costar number 3801) were used. Typically, cells achieved confluence after 5–6 days, and were studied 2–3 days later.

Phospholipid Overlay Assays—The peptide corresponding to the entire NHE1 cytosolic tail (residues 501–815 (44); cNHE1) was PCR cloned from rat kidney (forward primer: 5'-GATGGGATTCGCCCTGGTAGACCTGTTGGCT-3', reverse primer: 5'-GGGGAAGCTTCTCGAGTTCTCGAGTTCTACTGCCCTTTGGGGATGAA). The primers contained Xho/HindIII and BamHI sites, respectively, which permitted subcloning into a plasmid that added a His₆ tag to the N terminus. The peptide was purified to homogeneity by passage over Ni²⁺ columns and sequential dialysis to remove urea. The His₆-cNHE1 peptide was suspended in renaturing buffer containing 10 mM HEPES, pH 7, 150 mM NaCl, 5% glycerol, and 2 mM DDT. cNHE1 fusion protein (1 μg/ml) was then incubated for 1 h with membrane phospholipids spotted on nitrocellulose membranes (PIP strips, Echelon, Salt Lake City, UT), and probed for binding with either anti-NHE1 (45) or anti-His antibodies. Quantitative densitometric data were generated using a Storm phosphorimager and normalized to PI(4,5)P₂ intensity.

Surface Plasmon Resonance—Binding parameters for the interaction of phosphoinositides with the NHE1 cytosolic domain were measured using a Biacore 3000 SPR-based biosensor (Biacore AB, Uppsala, Sweden). cNHE1 peptide was prepared as previously described, and immobilized on the CM5 chip (Biacore) at a density of >1000 response units according to the manufacturer's protocol. Phospholipid analytes included 70% PC, 30% PS, which served as a control for inner leaflet phospholipids, and experimental groups comprised of C16- and diC₈-PI(4,5)P₂ or PI(3,4,5)P₃ (3% (w/w) in 70% PC, 30% PS), all of which were purchased from Echelon. Phospholipids were dispersed by sonication and passage through an extruder (Avanti Polar Lipids, Alabaster, AL). Different concentrations of phospholipid suspensions in Biacore HBS-P buffer (10 mM HEPES, pH 7.4, 150 mM NaCl, 0.005% surfactant P20) were flowed at 5 μl/min for 4 min to determine association rate constants, followed by a 4-min perfusion with buffer only to determine the dissociation rate constants. All data were corrected for the response obtained using a blank reference flow cell blocked with de-lipidated albumin (0.1 mg/ml). The chip surface was regenerated between experiments with 50 mM NaOH. Data were analyzed using the BIAevaluation 3.1 program as previously described (46).

Phosphoinositide Assays—Methods have previously been described (47, 48). LLC-PK1 cells were plated to obtain a density of 1.5 × 10⁶ cells/100-mm culture dish in DMEM/F-12 medium supplemented with 10% FBS and 1% penicillin/streptomycin. The medium was then replaced with phosphate-free DMEM supplemented with 0.2 mCi of ³²P_i (PerkinElmer Life Sciences NEX063) for 2 h at 37 °C (48, 49). Medium was replaced with buffer (110 mM KH₂PO₄ + 30 mM NaCl) containing 0.2 mCi of ³²P_i and 10 μM nigericin at experimental pH

values (6.5, 7.0, or 7.5) for 5 or 15 min. Cells were lysed with 1 M HCl containing 5 mM glacial acetic acid (250 μ l). Lipids were extracted in 665 μ l of chloroform and vortexed to uniformity. Aqueous and chloroform fractions were separated by centrifugation (1000 \times *g* for 5 min), and 50 μ l of the chloroform fraction was loaded as described below. As a positive control for PI(3,4,5)P₃, an *in vitro* lipid kinase assay was conducted (48). Briefly, 20 μ g of sonicated PI(4,5)P₂ (Echelon) substrate was added to the reaction assay buffer (10 mM Tris-Cl, pH 7.4, 150 mM NaCl, 5 mM EDTA, 100 μ M sodium orthovanadate). The reaction was started by adding 500 μ g of SF-9 purified PI 3-kinase- γ enzyme, 10 μ l of 440 μ M ATP, and 10 μ Ci of [γ -³²P]ATP (25 °C, 10 min) with continuous agitation, and stopped with 20 μ l of 6 N HCl. Lipids were extracted in 160 μ l of chloroform/methanol (1:1) followed by vortexing and centrifugation at 1000 \times *g* to separate the phases. Thirty μ l of the organic phase was spotted on 200- μ m silica-coated flexi-TLC plates (Selecto-flexible; Fischer Scientific) precoated with 1% potassium oxalate. Spots were dried and resolved chromatographically with 2 N glacial acetic acid, 1-propanol (1:1.87). Plates were dried after resolution, and exposed for autoradiography. PI(4,5)P₂ and PI(3,4,5)P₃ were quantified by densitometry and liquid scintillation counting.

Phospholipid Loading—Cells were cultured on permeable supports to generate polarized monolayers. To enhance specific phospholipid content, PI(4,5)P₂ or PI(3,4,5)P₃ vesicles, which have been chemically modified to resist phosphatase activity (Echelon), were incorporated into plasma membranes according to published methods (50, 51). For PI(4,5)P₂ analogs the phosphodiester bond is modified by addition of an α -fluorophosphonate moiety. For PI(3,4,5)P₃ analogs the 3-phosphate bond is rendered metabolically stable as a phosphorothioate. Phosphoinositide insertion into membrane domains was verified by immunodetection of GFP-tagged PLC δ or Akt pleckstrin homology (PH) domain peptides (see below).

Microscopy—Immunocytochemistry experiments were conducted according to previously described protocols (7). LLC-PK1 cells cultured on permeable supports were transiently transfected with GFP-conjugated PLC δ or Akt PH domain peptides using FuGENE6 reagent (Roche Applied Science). After 24–48 h cells were fixed in 4% paraformaldehyde, support membranes were removed with a scalpel, placed on coverslips, and examined with a Leica TCS SP2 confocal system. NHE1 and ZO-1 were localized in LLC-PK1 cells following incubation with rabbit polyclonal anti-NHE1 (1:500, 60 min, room temperature), followed by Texas Red-conjugated anti-rabbit IgG (1:200, 60 min, room temperature) and anti-ZO-1 (1:200, overnight, 4 °C), followed by AF488-conjugated goat anti-rat IgG (1:300, 60 min, room temperature). Digital images were processed with Molecular Devices deconvolution software version 9.1 and Adobe Photoshop version 9.0.

Total internal reflection fluorescence (TIRF) microscopy and fluorescence resonance energy transfer (FRET) measurements were performed using an Olympus IX71 Inverted Microscope configured for FRET (52) and equipped with a two-line Olympus TIRFM system and \times 60 TIRFM objective lens. TIRF BODIPY-PI(4,5)P₂ fluorescence was acquired using a multiargon laser with 488 nm excitation and 510 nm emission filters.

NHE1-PI(4,5)P₂ interactions within the plasma membrane were determined by combined TIRF/FRET using BODIPY-PI(4,5)P₂ (Avanti Polar Lipids) and RFP-NHE1 FRET donor/acceptor pairs. Images were acquired using a Hamamatsu ORCA-ER charge-coupled device (12 bit) controlled by SLIDE-BOOK software (Intelligent Imaging Innovations, Denver, CO). Image analyses were performed using ImageJ and involved subtraction of background autofluorescence and blurred light and quantification of fluorescence intensity. FRET was measured using the relative fluorescence intensity of the donor (BODIPY-PI(4,5)P₂, peak excitation/emission λ = 503/525), according to established methods (53). Calculation of FRET efficiency was performed using the equation, $E = 1 - F_{DA}/F_D$ (54), where F_{DA} is the fluorescence intensity of the donor BODIPY-PI(4,5)P₂ in cells expressing the acceptor RFP-NHE1, and F_D is the fluorescence intensity of the donor BODIPY-PI(4,5)P₂ in the absence of the acceptor RFP-NHE1. In control experiments with PI(4,5)P₂-BODIPY vesicles or cells expressing only RFP-NHE1, fluorescence values were unchanged over the pH 6.5–7.5 range, indicating that neither fluorophore was pH-sensitive.

Cytosolic pH Measurements—Spectrofluorimetric cytosolic pH assays in cell suspensions using BCECF-AM have been described previously (22, 45). Single cell pH assays were conducted in LLC-PK1 cells maintained on glass coverslips according to methods adapted from Bachmann *et al.* (55). Cells were transiently transfected with GFP-tagged PLC δ -PH or Akt-PH constructs. Fields containing cells with a plasma membrane fluorescence pattern, as well as GFP-transfected control cells, were isolated for examination at \times 40 magnification with a Leica DM IRE2 microscope. Cells were loaded *in situ* with BCECF-AM (Molecular Probes, Eugene, OR; 2.5 μ M, 15 min) \pm *N*-ethyl-*N*-isopropyl amiloride (EIPA, Sigma; 1 μ M), then incubated with NH₄Cl (30 mM in sodium-free Ringer solution, 20 min), acidified following a 90-s washout with sodium-free Ringer buffer, which was then replaced with Na⁺-containing Ringer buffer to allow Na⁺/H⁺ exchange. Cells were then observed for pH recovery, which was monitored by BCECF fluorescence (emission λ = 530 nm) following an 0.08-s excitation at λ = 495 and 440 nm every 20 s. Excitation pulses \leq 0.05 s yielded unacceptably low signal to background ratios, whereas \geq 0.12 s duration or more frequent pulses caused significant photobleaching. Calibration curves were generated with pH 6.0, 7.0, and 8.0 buffers in high K⁺, nigericin-permeabilized cells at the end of each experiment. Epifluorescence was recorded using a SPOT-RT camera (Diagnostic Instruments, Sterling Heights, MI) and images were acquired and analyzed using SimplePCI imaging software (Compix Inc., Cranberry Township, PA). Cytosolic pH was determined by calculating BCECF fluorescence ratios within a subcellular area that excluded plasma membrane and nuclei using SimplePCI software.

Apoptosis Assays—DNA degradation was employed as an index of apoptosis, and was assessed in fixed cells by nuclear morphology with DAPI labeling and TUNEL assays, according to previously described methods (7).

Immunoblot Analysis—Methods have previously been described (22). Briefly, cell monolayers were lysed and denatured in boiling buffer (125 mM Tris, pH 6.8, 2% SDS, 5% glyc-

Phosphoinositides Regulate NHE1

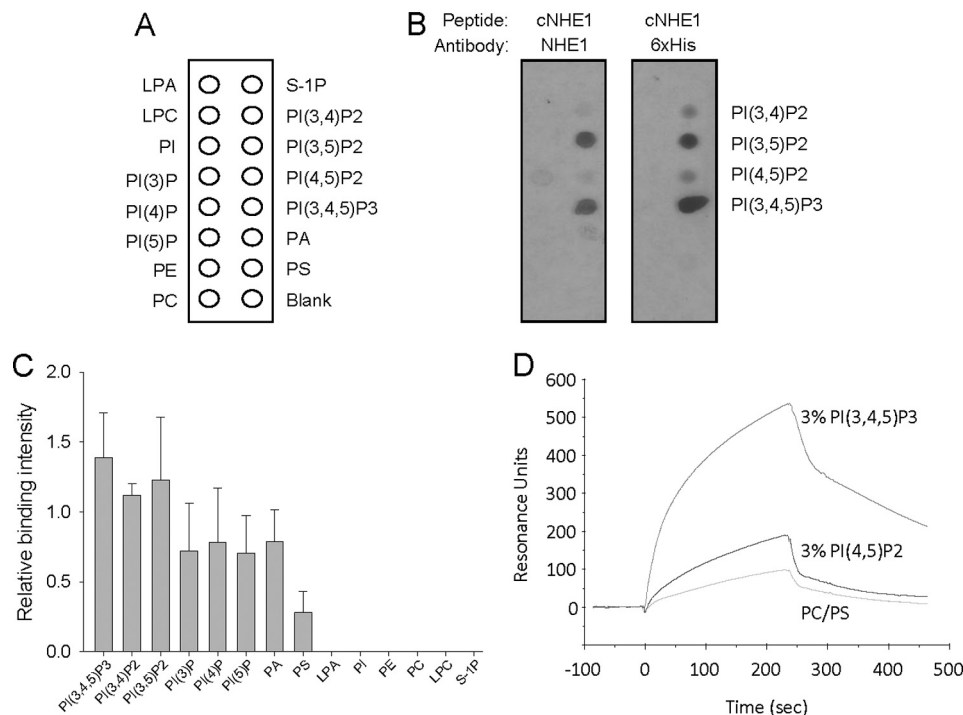


FIGURE 1. NHE1 binds multiple membrane lipids. Purified and renatured His₆-tagged cNHE1 was incubated with membrane phospholipids spotted on nitrocellulose membranes (A), and probed for binding with either anti-NHE1 or anti-His antibodies (B). C, quantitation of cNHE1 binding by densitometry, as determined by anti-NHE1 peptide antibody detection. Data are normalized to PI(4,5)P₂ binding (defined as 1.0 in each experiment). D, phospholipid binding to the immobilized cNHE1 peptide by surface plasmon resonance. 70% PC, 30% PS (50 μM) served as a control for inner leaflet phospholipids. Experimental groups include 50 μM C16-PI(4,5)P₂ or 50 μM C16-PI(3,4,5)P₃ (3% (w/w) in 70% PC, 30% PS vesicles). Phospholipids were dispersed by sonication and passage through an extruder. Analyte suspensions were flowed at 5 μl/min for 4 min to establish association, followed by a 4-min perfusion with buffer only, for dissociation.

erol, 1% β-mercaptoethanol, 0.003% bromphenol blue) for 5 min. Samples (20 μg of protein/lane) were resolved by SDS-PAGE and transferred to polyvinylidene difluoride (PVDF) membranes. Blots were blocked in 5% dried milk and 2% bovine serum albumin, probed with anti-active caspase-3 IgG (1:1,000, overnight, 4 °C), and then peroxidase-conjugated IgG (1:10,000, 1 h, room temperature). Band intensity was detected by enhanced chemiluminescence. Blots were stripped with 100 mM β-mercaptoethanol, 2% SDS, 62.5 mM Tris-HCl, pH 6.8, and then re-probed with anti-GAPDH IgG (1:3,000, 1 h, room temperature), followed by peroxidase-conjugated IgG (1:10,000, 1 h, room temperature).

Statistics—All data are representative of a minimum of three experiments per condition. Quantitative results are presented as mean ± S.E., unless otherwise indicated. Comparisons between multiple groups were made by one-way analysis of variance with the Student-Newman-Keuls, Kruskal-Wallis, or Dunnett tests for parametric and nonparametric data. Comparison between two groups was made by a paired *t* test. Statistical significance is defined as *p* < 0.05.

RESULTS

NHE1 Binds Multiple Membrane Phospholipids—PI(4,5)P₂ has previously been shown to bind NHE1 and regulate Na⁺/H⁺ exchange. Although PI(4,5)P₂ is relatively abundant, multiple other inner leaflet plasma membrane lipids could also potentially bind and influence NHE1 function. To test this possibility, membrane overlay assays were conducted with a His₆-tagged polypeptide corresponding to the entire cNHE1. The strips

were then probed with antibodies immunoreactive to either a cNHE1 peptide or the His₆ tag, revealing NHE1 binding most prominently to PI(3,4,5)P₃, and slightly less to the phosphatidylinositol (PI) bisphosphates (Fig. 1B). More prolonged exposure of blots to film revealed weaker cNHE1 binding to other membrane phospholipids, such as anionic PI monophosphates, phosphatidic acid, and rarely to PS (Fig. 1C and supplemental Fig. S1). Incubation with a His₆ peptide resulted in no binding, and His₆ peptide preincubation did not inhibit cNHE1 binding (not shown), indicating that the cNHE1-lipid interaction was not mediated by the His₆ tag.

To corroborate these findings and quantitatively characterize NHE1-phosphoinositide interactions, cNHE1 binding to PI(4,5)P₂ and PI(3,4,5)P₃ was tested with the surface plasmon resonance technique. Although PI(3,4)P₂ and PI(3,5)P₂ also bound avidly to cNHE1 (Fig. 1, B and C), experiments with these phosphoinositides were not pursued because they localize primarily to endosomes, rather than plasma membrane (56). To simulate physiologic conditions, C16-PI(4,5)P₂ or C16-PI(3,4,5)P₃ were mixed at 3% concentration (w/w) with lipid micelles containing 70% PC and 30% PS. Fig. 1D demonstrates a more rapid association and slower dissociation of PI(3,4,5)P₃ compared with PI(4,5)P₂ binding. PC/PS showed minimal binding, consistent with the overlay results.

Binding affinity constants were calculated using surface plasmon resonance and soluble C8-phosphoinositides, which permitted more accurate determination of phospholipid concen-

TABLE 1
Binding affinity constants for cNHE1 interactors

Data are expressed as mean \pm S.D.

cNHE1 interactor	k_{on} $M^{-1} s^{-1}$	k_{off} s^{-1}	K_d M
PI(4,5)P ₂	$0.9 \pm 0.5 \times 10^2$	$3.4 \pm 0.8 \times 10^{-3}$	$5.2 \pm 3.3 \times 10^{-5}$
PI(3,4,5)P ₃	$2.0 \pm 0.2 \times 10^2$	$4.8 \pm 1.5 \times 10^{-3}$	$2.5 \pm 1.0 \times 10^{-5}$
PI	No binding	No binding	No binding

trations. As seen in Table 1, PI(4,5)P₂ and PI(3,4,5)P₃ each bound with low affinity to cNHE1. PI(3,4,5)P₃ affinity was relatively greater compared with PI(4,5)P₂, in agreement with the overlay and C16-phosphoinositide surface plasmon resonance studies. As a negative control, cNHE1 did not bind PI.

NHE1 Binds Phosphoinositides through Electrostatic Interactions—To test the mechanism of NHE1-phosphoinositide interaction, wild-type and cNHE1 mutant peptide (Fig. 2A) binding was tested by two different methods. Fig. 2B demonstrates complete abrogation of membrane phospholipid binding to the cNHE1 peptide containing combined M1 + M2 mutations, by surface plasmon resonance, consistent with a prior report that both polybasic NHE1 domains are required for PI(4,5)P₂ binding (29). Absence of M1 + M2 peptide association with PI(4,5)P₂ or PI(3,4,5)P₃ was confirmed by lipid overlay assays (Fig. 2C). To determine the relative contribution of each polybasic NHE1 domain to phosphoinositide binding, membrane overlay assays were conducted with 513–520 (M1) or 556–564 (M2) NHE1 mutant peptides. These experiments demonstrated equivalent phospholipid binding between both mutants (Fig. 2C), which was not different compared with wild-type NHE1 binding. These results indicate that positively charged amino acids within each domain are required for phosphoinositide binding.

Effect of pH on NHE1-Phosphoinositide Binding—Multiple stimuli cause rapid Na⁺/H⁺ exchange, which alters pH in the microenvironment of the NHE1 cytosolic tail. To determine whether local pH modulation affects the NHE1-phosphoinositide interaction, surface plasmon resonance experiments were conducted at varying pH values within the physiologic range. Fig. 3, A and B, show enhanced NHE1 association with PI(4,5)P₂ and PI(3,4,5)P₃ with progressive acidification of binding buffer *in vitro*, suggesting that intracellular acidosis may amplify NHE1 activity by promoting interactions between the exchanger and nearby membrane phosphoinositides.

To verify the effect of cytosolic pH on NHE1-PI(4,5)P₂ binding in live cells, plasma membrane interactions were determined by combined TIRF/FRET using BODIPY-PI(4,5)P₂ and RFP-NHE1 FRET donor/acceptor pairs. Plasma membrane NHE1 and PI(4,5)P₂ are shown by TIRF microscopy (Fig. 3C). At pH 6.5, the fluorescence intensity of BODIPY-PI(4,5)P₂ was decreased in cells expressing RFP-NHE1 (Fig. 3C) due to a FRET signal between the donor and acceptor, confirming their interaction in the plasma membrane (Fig. 3D). FRET was abrogated by increasing pH (Fig. 3D) as seen by no change in the BODIPY-PI(4,5)P₂ fluorescence in cells expressing RFP-NHE1 (Fig. 3C). The data suggest that the plasma membrane PI(4,5)P₂-NHE1 interaction occurs under acidic conditions, whereas negligible FRET at higher pH is consistent with the quiescent state of NHE1 under ambient conditions. Alteration

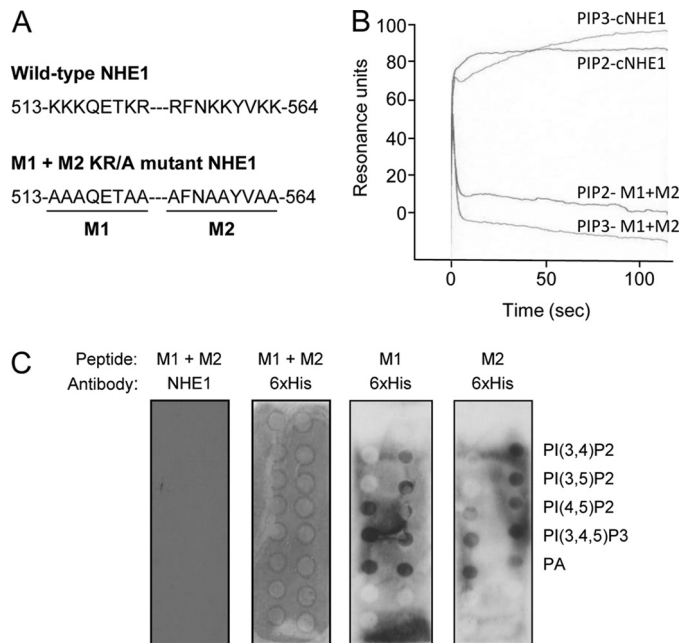


FIGURE 2. NHE1 binds phosphoinositides through electrostatic interactions. Association of diC₈-PI(4,5)P₂ and diC₈-PI(3,4,5)P₃ with wild-type and mutant cNHE1 peptides (mutated residues are shown in A), as measured by surface plasmon resonance (B). Mutant cNHE1 binding to phospholipids, by membrane overlay assays (C). In control experiments binding to phosphatidylinositol monophosphates in the absence of cNHE1 peptides was occasionally observed (not shown), indicating a lack of binding specificity to these sites.

of cytosolic pH over the physiologic range and duration of NHE1 activity experiments (see Fig. 5) had no effect on cellular PI(4,5)P₂ or PI(3,4,5)P₃ content (supplemental Fig. S2).

PI(4,5)P₂, PI(3,4,5)P₃, and NHE1 Co-localize to Lateral Membrane Domains—To determine the functional consequences of PI(4,5)P₂ and PI(3,4,5)P₃ binding to NHE1, we first determined whether the phosphoinositides sorted to the proper membrane domains for interaction with NHE1, which localizes to the basolateral surface in proximal tubule (18). Purified PI(4,5)P₂ and PI(3,4,5)P₃ were added to polarized LLC-PK1 PTC expressing GFP-tagged PLC δ -PH and Akt-PH, which fluorescently label PI(4,5)P₂ and PI(3,4,5)P₃, respectively. These experiments demonstrated that PI(4,5)P₂ were sorted primarily to apical and lateral membranes (supplemental Fig. 3, A and D), whereas PI(3,4,5)P₃ was localized to lateral membranes (supplemental Fig. S3, B and E), consistent with reports in other epithelia (50, 51). As expected, NHE1 localized to the basolateral membrane in LLC-PK1 cells (supplemental Fig. 3, C and F).

To test whether NHE1 and phosphoinositides co-localize *in vivo*, polarized LLC-PK1 cells were co-labeled for endogenous NHE1, PI(4,5)P₂, PI(3,4,5)P₃, and ZO-1 (to demarcate apical-lateral junctions) and visualized by confocal microscopy. Fig. 4 indicates, that in the X-Y plane, NHE1 co-localized with PI(4,5)P₂ (Fig. 4, A–C) and PI(3,4,5)P₃ (Fig. 4, D–F) at lateral membranes. Images in the X-Z plane demonstrate predominant NHE1 co-localization with PI(4,5)P₂ (Fig. 4, G–J) and PI(3,4,5)P₃ (Fig. 4, K–N) to regions below ZO-1, suggesting that PI(4,5)P₂ and PI(3,4,5)P₃ interact with NHE1 at the lateral membrane.

Phosphoinositides Regulate NHE1

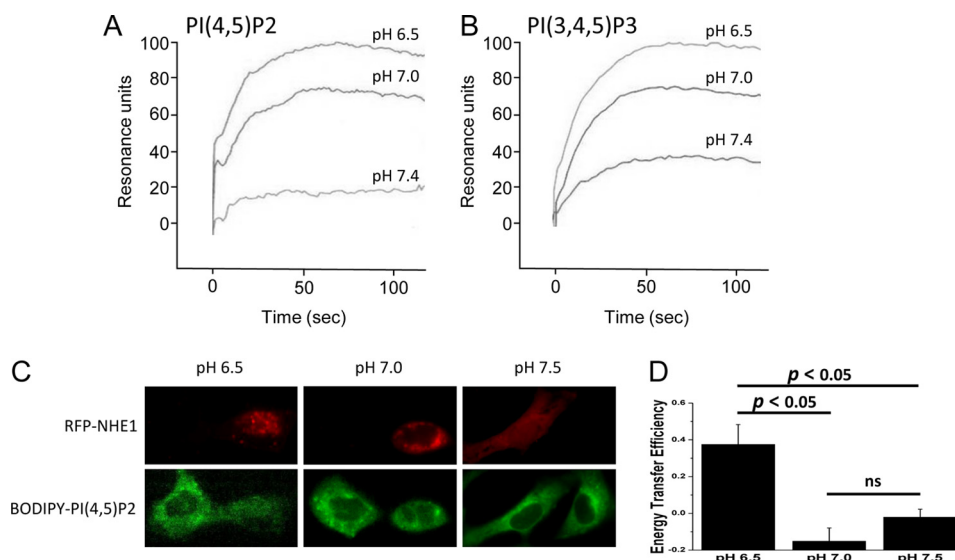


FIGURE 3. Effect of pH on NHE1-phosphoinositide binding. NHE1 association with diC₈-PI(4,5)P₂ (A) and diC₈-PI(3,4,5)P₃ (B) at varying pH values within the physiologic range. Dissociation rates were not significantly different between pH conditions (not shown). Note that the initial, steep curves are a result of bulk solute shift, rather than specific binding. C, representative epifluorescence images of RFP-NHE1-transfected and untransfected cells and corresponding TIRF images of BODIPY fluorescence. Cytosolic pH was clamped at pH 6.5, 7.0, and 7.5 following exposure to nigericin (10 μM, 15 min) in 100 mM KH₂PO₄ + 30 mM NaCl buffer. D, energy transfer efficiency between PI(4,5)P₂-BODIPY (donor) and RFP-NHE1 (acceptor) measured by TIRF microscopy. Data are expressed as mean ± S.E. from three experiments, 8–10 pairs of cells within the same microscopic field per experiment.

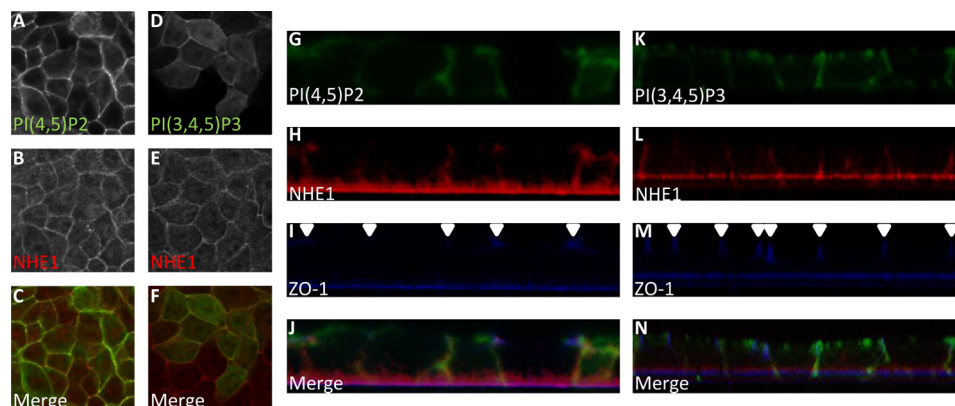


FIGURE 4. PI(4,5)P₂, PI(3,4,5)P₃, and NHE1 co-localize to lateral membrane domains. LLC-PK1 cells were polarized on permeable supports and transiently transfected with GFP-tagged PLCδ (A–F and K–N) or Akt (D–F and K–N) PH domain peptide cDNAs. NHE1 distribution was determined immunocytochemically with anti-NHE1, followed by Texas Red-conjugated anti-rabbit IgG (B, E, H, and L). Apical-basolateral junctions were labeled with ZO-1 antibodies, followed by AF488-conjugated goat anti-rat IgG (I and M, demarcated with arrowheads for clarity). Phosphoinositide, NHE1, and ZO-1 localization were detected in paraformaldehyde-fixed cells by confocal microscopy, and displayed in the X–Y (A–F) and X–Z plane (G–N).

PI(4,5)P₂ and PI(3,4,5)P₃ Divergently Regulate NHE1-dependent Na⁺/H⁺ Exchange—To assess the effect of phosphoinositides on NHE1 function, EIPA-inhibitable Na⁺/H⁺ transport activity was assayed in LLC-PK1 cells following incorporation with added PI(4,5)P₂ or PI(3,4,5)P₃. Fig. 5A reveals that PI(4,5)P₂-loaded cells enhanced NHE1-dependent Na⁺/H⁺ exchange, whereas PI(3,4,5)P₃ surprisingly inhibited Na⁺/H⁺ transport (Fig. 5, A and B). To confirm these results, NHE1 activity was determined in LLC-PK1 cells preincubated with neomycin, which sequesters PI(4,5)P₂. These studies resulted in >50% inhibition of NHE1-dependent Na⁺/H⁺ exchange (Fig. 5A). To corroborate the effects of PI(3,4,5)P₃, NHE1 activity was measured in cells preincubated with LY-294002 or wortmannin, both of which inhibit PI 3-kinase activity and PI(3,4,5)P₃ generation. These experiments showed that PI 3-kinase inhibition enhanced NHE1 activity (Fig. 5A), consistent with PI(3,4,5)P₃ modulation of NHE1.

Phosphoinositide effects on NHE1-regulated Na⁺/H⁺ exchange were further tested using a different strategy, in which PI(4,5)P₂ and PI(3,4,5)P₃ were selectively sequestered in LLC-PK1 cells expressing PH domain-containing PLCδ and Akt peptides (57), respectively. NHE1 activity was then assessed in individual adherent cells following recovery from an acid load, by fluorescence microscopy (Fig. 5, C–E). Similar NHE1 activity was observed in polarized cells maintained on permeable supports (2.12 ± 0.33 × 10⁻³ pH units/s, and supplemental Fig. S4). Fig. 5D demonstrates that PI(4,5)P₂ sequestration resulted in slower cytosolic pH recovery compared with GFP-transfected control cells (Fig. 5C). In most PLCδ-expressing cells cytosolic pH never reached baseline values. On the other hand, PI(3,4,5)P₃ blockade enhanced NHE1-dependent Na⁺/H⁺ transport (Fig. 5E). Quantification from the single cell pH experiments is shown in Fig. 5F. The results indicate that, although PI(4,5)P₂ and PI(3,4,5)P₃ each bind the NHE1 cytosol-

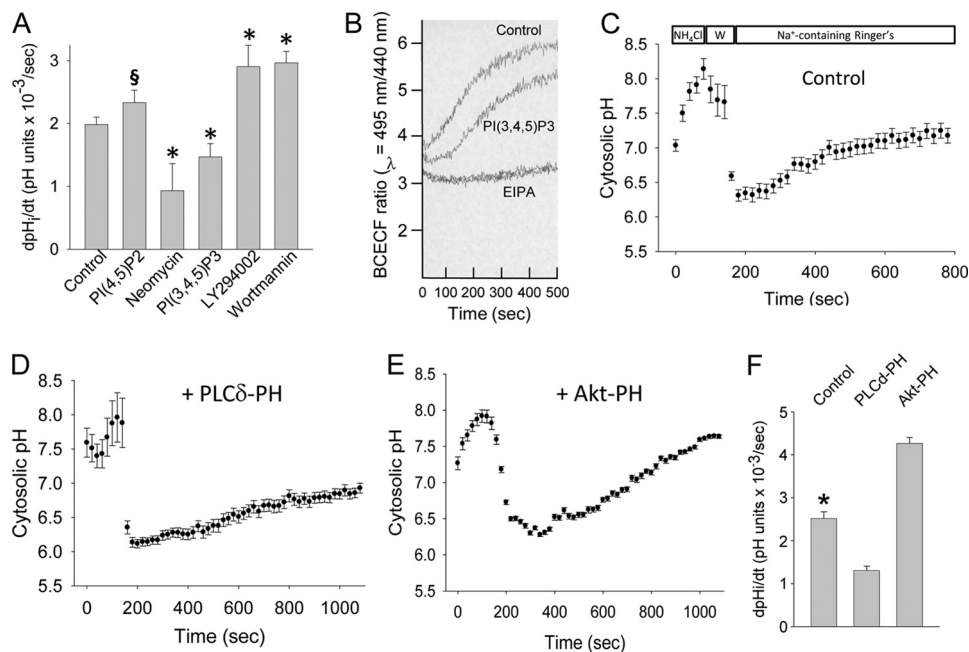


FIGURE 5. PI(4,5)P₂ and PI(3,4,5)P₃ differentially regulate NHE1-dependent Na⁺/H⁺ exchange. *A*, LLC-PK1 cells were preincubated with metabolically stable (phosphatase-resistant) diC₈-PI(4,5)P₂ or diC₈-PI(3,4,5)P₃, PI(4,5)P₂ inhibitor neomycin, or PI 3-kinase inhibitors LY-294002 (20 μM, 30 min, 37 °C) or wortmannin (100 nM, 30 min, 37 °C). Maximum EIPA (1 μM)-inhibitable Na⁺/H⁺ exchange was determined in response to cytosolic acidification following NH₄Cl washout. Cytosolic pH was determined by BCECF fluorescence, and measured by spectrofluorimetry. Results from four to six experiments per condition are shown. *, *p* < 0.05 and §, *p* = 0.12 compared with control group by analysis of variance on ranks with the Dunnett post hoc test. *B*, representative pH recovery tracing from one experiment in PI(3,4,5)P₃-loaded versus control cells. *C–E*, NHE1-dependent (EIPA (1 μM)-inhibitable) Na⁺/H⁺ exchange was measured in individual, BCECF-loaded LLC-PK1 cells by fluorescence microscopy following NH₄Cl washout (*W* in *C*). Mean values from three experiments, 35–50 cells per experiment, are shown for GFP-transfected (*C*), GFP-tagged PLCδ-PH-expressing (*D*), and GFP-tagged Akt-PH-expressing (*E*) cells. Maximum rates of EIPA-inhibitable Na⁺/H⁺ exchange are summarized in *F*. *, *p* < 0.05 compared with other groups by analysis of variance.

lic tail, the phosphoinositides exert opposite effects on exchanger activity.

PI(4,5)P₂ and PI(3,4,5)P₃ Differentially Regulate Apoptosis—We have previously shown that NHE1 activity inhibits PTC apoptosis (22, 45, 58). To determine the effect of phosphoinositides, PI(4,5)P₂ and PI(3,4,5)P₃ were separately incorporated in LLC-PK1 cells, which were then stimulated to undergo apoptosis with staurosporine or cisplatin. Fig. 6*A* shows that PI(4,5)P₂ blunted apoptosis, in agreement with its anti-apoptotic effects in other systems (21), whereas PI(3,4,5)P₃ had no effect. Similar results were observed in cisplatin-stimulated LLC-PK1 cells, (Fig. 6*B*).

PI(4,5)P₂ and PI(3,4,5)P₃ Differentially Regulate NHE1-dependent Cell Survival—To address the role of phosphoinositides on NHE1-regulated cell survival, apoptosis was assessed in LLC-PK1 cells expressing PI(4,5)P₂ and PI(3,4,5)P₃ neutralizing peptides, PLCδ-PH and Akt-PH. As observed in Fig. 7*A*, sequestration of PI(4,5)P₂, and to a lesser extent PI(3,4,5)P₃, modulated apoptosis. EIPA inhibition of NHE1 yielded no additive effect on apoptosis in cells expressing PLCδ, suggesting that the NHE1-PI(4,5)P₂ interaction is a major mechanism of cell survival.

Interpretation of the PI(3,4,5)P₃ data is complicated because PI(3,4,5)P₃ simultaneously inhibits anti-apoptotic NHE1 activity, and serves as a docking site for the pro-survival kinase, Akt. To clarify the link between PI(3,4,5)P₃ and NHE1, apoptosis was measured in wild-type mouse PTC in the presence of PI 3-kinase and Akt inhibitors. As expected, inhibition of Akt enhanced apoptosis in wild-type RTC (Fig.

7*B*). However, combined Akt plus PI 3-kinase inhibition did not increase apoptosis as significantly. Preincubation with the amiloride derivative EIPA, at a concentration specific for NHE1 inhibition (1 μM), significantly enhanced apoptosis (Fig. 7*B*), highlighting the importance of NHE1 function in cell survival.

To confirm the role of phosphoinositides upon NHE1-regulated cell survival, experiments were repeated in NHE1-deficient Swe/Swe cells. Staurosporine-induced apoptosis was modestly enhanced in Swe/Swe (Fig. 7*C*) compared with wild-type (Fig. 7*B*) cells. In contrast to wild-type cells, no difference in apoptosis was noted in Swe/Swe cells preincubated with Akt versus Akt plus PI 3-kinase inhibitors (Fig. 7*C*), indicating that the PI(3,4,5)P₃ interaction with NHE1 is nearly as potent for stimulating apoptosis as the absence of NHE1. As a negative control, no additional apoptosis was observed following EIPA co-incubation.

The findings with PI 3-kinase and Akt inhibitors were corroborated by experiments in wild-type and Swe/Swe mouse PTC loaded with phosphoinositides, which were then induced to undergo apoptosis by staurosporine (Fig. 7, *D–G*) or cisplatin (supplemental Fig. S5). Apoptosis was measured by TUNEL and activated caspase-3 assays. Importantly, enhanced apoptosis observed in Swe/Swe cells exposed to either staurosporine or cisplatin was unaffected by PI(4,5)P₂ or PI(3,4,5)P₃ supplementation, suggesting that the interaction between NHE1 and phosphoinositides regulates cell survival.

Phosphoinositides Regulate NHE1

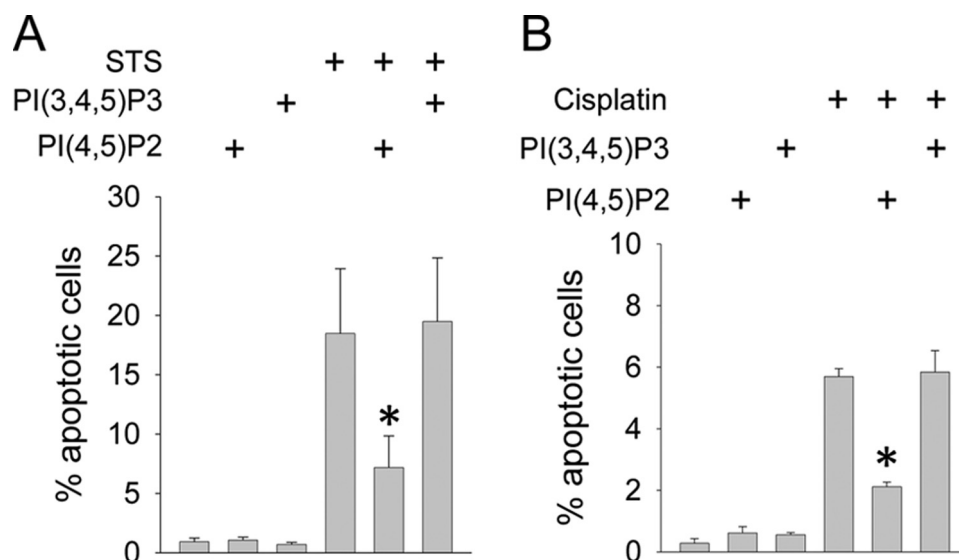


FIGURE 6. **PI(4,5)P₂ and PI(3,4,5)P₃ differentially regulate apoptosis.** LLC-PK1 cells were maintained on permeable supports, and pre-treated by incorporation of metabolically stable diC₈-PI(4,5)P₂ or diC₈-PI(3,4,5)P₃. Cells were then induced to undergo apoptosis with staurosporine (STS, 1 μ M, 5 h, in panel A) or cisplatin (25 μ M, 18 h, 37 $^{\circ}$ C, in panel B). Apoptosis was quantified by TUNEL. Note the difference in y-axis scale between histograms. *, $p < 0.05$ compared with staurosporine-only or cisplatin-only groups by analysis of variance.

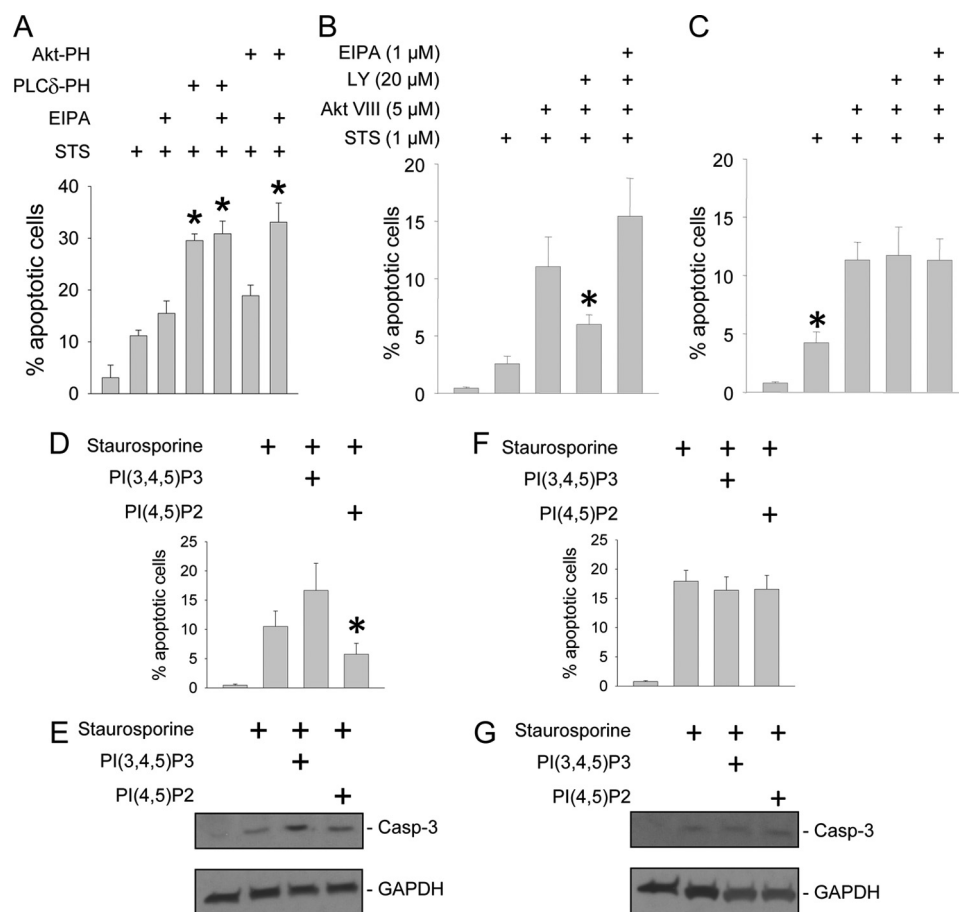


FIGURE 7. **PI(4,5)P₂ and PI(3,4,5)P₃ differentially regulate NHE1-dependent cell survival.** LLC-PK1 cells (A), as well as wild-type (B, D, and E) and NHE1-null mouse proximal tubule cell lines (C, F, and G) were cultured on permeable supports. LLC-PK1 cells underwent PI(4,5)P₂ or PI(3,4,5)P₃ sequestration by overexpressing GFP-tagged PLC δ -PH or Akt-PH peptide constructs, respectively (A), or preincubation with PI 3-kinase inhibitor LY-294002, Akt inhibitor Akt VIII, or NHE1 inhibitor EIPA (B and C). Mouse PTC were loaded with PI(4,5)P₂ or PI(3,4,5)P₃ vesicles (D–G). All groups were induced to undergo apoptosis with staurosporine (STS, 1 μ M, 5 h, 37 $^{\circ}$ C). Apoptosis was determined by TUNEL assay (A–D and F) or detection with antibodies that recognize the active, 17 kDa, cleaved caspase-3 by immunoblot analysis (E and G, upper panels). Blots were stripped and re-probed for GAPDH as a loading control (E and G, lower panels). *, $p < 0.05$ compared with STS alone by analysis of variance on ranks and the Dunnett post hoc analysis in A; *, $p < 0.05$ compared with all other groups by analysis of variance in B–D.

DISCUSSION

We previously demonstrated that the NHE1 Na^+/H^+ exchanger is instrumental in defending against PTC apoptotic stress, but the regulatory mechanisms had not been elucidated. We now describe molecular interactions between the NHE1 cytosolic tail and multiple membrane phospholipids, most notably polyvalent phosphoinositides. These data are largely consistent with previous studies showing that $\text{PI}(4,5)\text{P}_2$ binds to NHE1 and stimulates Na^+/H^+ exchange (29).

The 25–50 μM binding affinity between $\text{PI}(4,5)\text{P}_2$ or $\text{PI}(3,4,5)\text{P}_3$ and NHE1 is in agreement with estimated membrane $\text{PI}(4,5)\text{P}_2$ concentrations of at least 10–15 μM (36–38). $\text{PI}(3,4,5)\text{P}_3$ content is estimated to be an order of magnitude less than $\text{PI}(4,5)\text{P}_2$ under basal conditions, but can increase by 15-fold in response to agonist and PI 3-kinase stimulation (59). Such low affinity binding is purported to be physiologically relevant, by facilitating rapid on-off modulation of target proteins, in contrast to higher affinity interactions, which tend to be irreversible (35). Further evidence of significance can be extrapolated from a recent screen for inhibitors of PH domain binding to $\text{PI}(3,4,5)\text{P}_3$, which yielded peptides with IC_{50} values of 30–40 μM and *in vivo* activity (60). Unlike PH domain-containing proteins, which typically bind phosphoinositides with 1:1 stoichiometry, proteins with polybasic motifs, like NHE1, bind in a multivalent manner to regions of high phosphoinositide density (61, 62). We propose that focal, enhanced concentrations of NHE1 and phosphoinositides promote discrete, low affinity electrostatic interactions, which regulate exchanger activity.

The mechanism of NHE1-phosphoinositide association appears to be through electrostatic interaction, as evidenced by the absence of phospholipid binding to NHE1 constructs containing KR/A mutations within two juxtamembrane sites. We and others (29)³ have shown that the M1 + M2 mutant exhibits diminished Na^+/H^+ exchange activity. Basic residues within each domain were required for phosphoinositide binding, confirming a prior report for NHE1 (29), and consistent with recent Kir2 channel- $\text{PI}(4,5)\text{P}_2$ data (63, 64). Anionic regions of other proteins, such as ezrin/radixin/moesin also interact with these same cationic NHE1 residues (22, 65), highlighting the notion that multiple proteins and lipids could cooperatively regulate NHE1.

Because NHE1 mediates H^+ extrusion, we tested the effect of pH on the NHE1-phosphoinositide interaction. Binding was optimum at pH 6.5, and lessened with progressive alkalinity, consistent with observations that both acidification and $\text{PI}(4,5)\text{P}_2$ binding facilitate Na^+/H^+ exchange, and $\text{PI}(4,5)\text{P}_2$ binding to other proteins is amplified at low pH (66). However, pH changes of this magnitude are unlikely to significantly alter binding to KR residues, which have very high $\text{p}K_a$, and charge should therefore remain unchanged in the physiologic pH range. On the other hand, histidine has a $\text{p}K_a$ of 6.5–7.5, and a ⁵⁴⁴HYGHHH⁵⁴⁹ motif between the KR-rich binding sites has been implicated in NHE1 regulation (67). Histidine protonation could therefore be responsible for minor modulation in

observed phosphoinositide binding, either through direct interaction or by altering the polypeptide structure to expose distant binding sites. This is particularly plausible because curve fitting programs indicated that NHE1-phosphoinositide dissociation was not entirely logarithmic (not shown), and suggested a two-component process.

A somewhat surprising finding was the divergent effects of $\text{PI}(4,5)\text{P}_2$ versus $\text{PI}(3,4,5)\text{P}_3$ on NHE1 function, despite similar binding mechanisms and affinity. Most ion channels and exchangers are equally regulated by multiple phosphoinositides, although inwardly rectifying K^+ channels (particularly Kir2.1) are also differentially regulated by $\text{PI}(4,5)\text{P}_2$ and $\text{PI}(3,4,5)\text{P}_3$ (25). $\text{PI}(4,5)\text{P}_2$ allosterically regulates Kir2 pore opening through binding to specific and nonspecific sites, which become exposed and dock only after significant $\text{PI}(4,5)\text{P}_2$ -induced modulation of the channel structure occurs (63, 64). Although the major NHE1 binding domains appear to be the juxtamembrane and cytosolic polybasic motifs, we speculate that induced NHE1 conformational changes could similarly create minor binding sites that distinguish $\text{PI}(4,5)\text{P}_2$ from $\text{PI}(3,4,5)\text{P}_3$. Isolated effects of $\text{PI}(4,5)\text{P}_2$ versus $\text{PI}(3,4,5)\text{P}_3$ had not previously been explored in detail, but prior studies demonstrated $\text{PI}(4,5)\text{P}_2$ stimulation of NHE1, and suggested a neutral role for $\text{PI}(3,4,5)\text{P}_3$ (29, 30). Reconciliation of the $\text{PI}(3,4,5)\text{P}_3$ findings with ours is not obvious, although methods for phosphoinositide introduction, NHE1 stimulation, and Na^+/H^+ exchange measurements markedly differed between studies.

The possibility of NHE1 binding to PS was explored because PS is negatively charged, and PS flipping from the inner to outer plasma membrane leaflet during apoptosis would result in loss of interaction with the NHE1 cytosolic tail. However, significant binding was not observed between NHE1 and PS. A recent report demonstrated that a different C-terminal NHE1 peptide lipid-interacting domain (residues 542–598) bound multiple membrane phospholipids, including PS, using a different assay (31). Our data indicate that the N-terminal charged residues, some of which were deleted from the lipid-interacting domain, may be important for discriminating NHE1-phospholipid binding. However, because vesicles used for our phosphoinositide binding experiments contained 30% PS we cannot exclude the possibility that PS and phosphoinositides may cooperatively bind and regulate NHE1 function, as recently demonstrated for Akt (68).

Because of homology between NHE isoforms, similar regulation by phospholipids might be anticipated. However, in contrast to NHE1, interaction between the NHE3 C terminus and $\text{PI}(3,4,5)\text{P}_3$ enhanced Na^+/H^+ exchange (28, 30, 69), whereas conflicting effects of $\text{PI}(4,5)\text{P}_2$ on NHE3 were described (28, 30). Moreover, opposite NHE1 and NHE3 activities were observed in response to cell volume perturbations (70–73), which may be a relevant stimulus with apoptosis, and suggest that phosphoinositide interactions may regulate Na^+/H^+ exchange in an isoform-specific manner.

Based upon our current and previously published data (21, 22, 45) we propose a model in which $\text{PI}(4,5)\text{P}_2$ and $\text{PI}(3,4,5)\text{P}_3$, the major phosphoinositides within the plasma membrane inner leaflet, form an on-off switch to regulate NHE1 (Fig. 8).

³ S. Khan and J. R. Schelling, unpublished observations.

Phosphoinositides Regulate NHE1

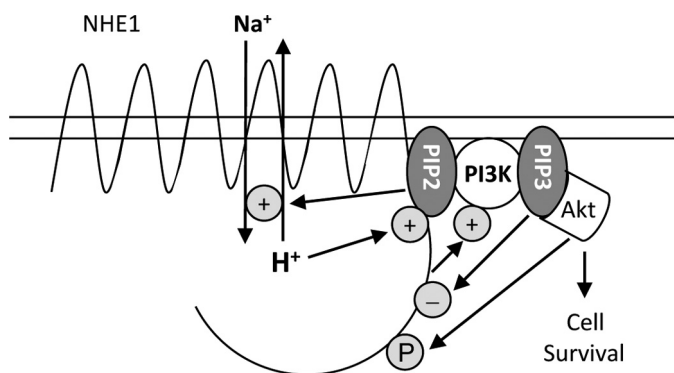


FIGURE 8. Schematic diagram summarizing the role of phosphoinositides on regulation of NHE1-dependent cell survival. In response to apoptotic stress, NHE1 is initially stimulated by PI(4,5)P₂ binding to mediate cytoprotection. NHE1 then indirectly activates PI 3-kinase to phosphorylate PI(4,5)P₂. The resulting PI(3,4,5)P₃ dually stimulates sustained downstream Akt survival signaling, and negatively feeds back to dampen NHE1 activity through competitive inhibition, as well as depletion of PI(4,5)P₂ pools.

The PI(4,5)P₂-NHE1 interaction promotes NHE1 activity, and is consistent with anti-apoptotic roles of both molecules. The relatively greater magnitude of the PI(4,5)P₂ effect on apoptosis, compared with NHE1-regulated Na⁺/H⁺ exchange, suggests that PI(4,5)P₂-dependent cytoprotection is mediated by additional, NHE1-independent mechanisms. We have previously shown that NHE1 activation stimulates PI 3-kinase (22), which leads to Akt activation. Two groups have shown that NHE1 Ser⁶⁴⁸ is an Akt substrate (74, 75), although the ramifications are unclear, because opposite effects of Ser⁶⁴⁸ phosphorylation on NHE1 activity were observed.

In contrast to the straightforward interpretation of the NHE1-PI(4,5)P₂ interaction on cell survival, the role of PI(3,4,5)P₃ is complex, because it potentially promotes apoptosis through NHE1 inhibition, as well as anti-apoptosis by docking PDK1 and Akt. This dichotomy is best illustrated by the different consequences of PI(3,4,5)P₃ modulation in wild-type *versus* NHE1-null cell lines (Fig. 7). PI 3-kinase inhibition lessened apoptosis in wild-type, but not in NHE1-null cells. Conversely, loading cell membranes with PI(3,4,5)P₃ enhanced apoptosis in wild-type, but not NHE1-null cells, indicating that the isolated effect of PI(3,4,5)P₃ binding to NHE1 is to facilitate apoptosis. However, the kinetics of PI(3,4,5)P₃-effector interactions differ. NHE1 activity is induced within seconds, which stimulates downstream PI 3-kinase activity (22). NHE1 activity recedes by 3–5 min, which coincides with Akt release to the cytosol (76), where Akt activity peaks at 30–60 min (22). Therefore, we propose that initially, concomitant NHE1 and PI(3,4,5)P₃-mediated Akt activation support cell survival. After Akt release, PI(3,4,5)P₃ would become available to bind and modulate NHE1, ensuring that the exchanger returns to its quiescent state.

The results are consistent with an on-off switch mechanism of NHE1 regulation, whereby the exchanger toggles between low affinity interactions with PI(4,5)P₂ and PI(3,4,5)P₃. In response to cytosol acidification and/or apoptotic stress, NHE1 interaction with PI(4,5)P₂ is enhanced, which mediates cytoprotection. NHE1 stimulation leads to activation of PI 3-kinase, which phosphorylates PI(4,5)P₂. The resulting PI(3,4,5)P₃ initially stimulates downstream Akt survival signaling, and subse-

quently competes with reduced levels of PI(4,5)P₂ for binding to NHE1, which dampens its activity.

Acknowledgments—We are grateful to Dr. John Orlowski (McGill University), who supplied the NHE1 mutant constructs, Dr. Tamas Balla (NIH-NICHD), who supplied the PLCδ-PH and Akt-PH constructs, and Dr. Josette Noel (University of Montreal), who supplied the NHE1 antibodies.

REFERENCES

- Coresh, J., Selvin, E., Stevens, L. A., Manzi, J., Kusek, J. W., Eggers, P., Van Lente, F., and Levey, A. S. (2007) *JAMA* **298**, 2038–2047
- Collins, A. J., Foley, R. N., Herzog, C., Chavers, B. M., Gilbertson, D., Ishani, A., Kasiske, B. L., Liu, J., Mau, L. W., McBean, M., Murray, A., St. P. W., Guo, H., Li, Q., Li, S., Li, S., Peng, Y., Qiu, Y., Roberts, T., Skeans, M., Snyder, J., Solid, C., Wang, C., Weinhandl, E., Zaun, D., Arko, C., Chen, S. C., Dalleska, F., Daniels, F., Dunning, S., Ebben, J., Frazier, E., Hanzlik, C., Johnson, R., Sheets, D., Wang, X., Forrest, B., Constantini, E., Everson, S., Eggers, P. W., and Agodoa, L. (2010) *Am. J. Kidney Dis.* **55**, S1–S7
- Risdon, R. A., Sloper, J. C., and De Wardener, H. E. (1968) *Lancet* **2**, 363–366
- Schainuck, L. I., Striker, G. E., Cutler, R. E., and Benditt, E. P. (1970) *Hum. Pathol.* **1**, 631–641
- Bohle, A., Muller, G. A., Wehrmann, M., Mackensen-Haen, S., and Xiao, J. C. (1996) *Kidney Int.* **54**, S2–S9
- Bunnag, S., Einecke, G., Reeve, J., Jhangri, G. S., Mueller, T. F., Sis, B., Hidalgo, L. G., Mengel, M., Kayser, D., Kaplan, B., and Halloran, P. F. (2009) *J. Am. Soc. Nephrol.* **20**, 1149–1160
- Schelling, J. R., Nkemere, N., Kopp, J. B., and Cleveland, R. P. (1998) *Lab. Invest.* **78**, 813–824
- Khan, S., Cleveland, R. P., Koch, C. J., and Schelling, J. R. (1999) *Lab. Invest.* **79**, 1089–1099
- Schelling, J. R., and Cleveland, R. P. (1999) *Kidney Int.* **56**, 1313–1316
- Ortiz, A. (2000) *Kidney Int.* **58**, 467–485
- Kumar, D., Robertson, S., and Burns, K. D. (2004) *Mol. Cell. Biochem.* **259**, 67–70
- Susztak, K., Ciccone, E., McCue, P., Sharma, K., and Böttinger, E. P. (2005) *PLoS Med.* **2**, e45
- Lagadic-Gossmann, D., Huc, L., and Lecreur, V. (2004) *Cell Death Differ.* **11**, 953–961
- Matsuyama, S., Llopis, J., Deveraux, Q. L., Tsien, R. Y., and Reed, J. C. (2000) *Nat. Cell Biol.* **2**, 318–325
- Segal, M. S., and Beem, E. (2001) *Am. J. Physiol. Cell Physiol.* **281**, C1196–C1204
- Antonsson, B., Conti, F., Ciavatta, A., Montessuit, S., Lewis, S., Martinou, I., Bernasconi, L., Bernard, A., Mermoud, J. J., Mazzei, G., Maundrell, K., Gambale, F., Sadoul, R., and Martinou, J. C. (1997) *Science* **277**, 370–372
- Verhagen, A. M., Ekert, P. G., Pakusch, M., Silke, J., Connolly, L. M., Reid, G. E., Moritz, R. L., Simpson, R. J., and Vaux, D. L. (2000) *Cell* **102**, 43–53
- Biemesderfer, D., Reilly, R. F., Exner, M., Igarashi, P., and Aronson, P. S. (1992) *Am. J. Physiol.* **263**, F833–F840
- Barber, D. L. (1991) *Cell Signal.* **3**, 387–397
- Wakabayashi, S., Shigekawa, M., and Pouyssegur, J. (1997) *Physiol. Rev.* **77**, 51–74
- Schelling, J. R., and Abu Jawdeh, B. G. (2008) *Am. J. Physiol. Renal Physiol.* **295**, F625–F632
- Wu, K. L., Khan, S., Lakhe-Reddy, S., Jarad, G., Mukherjee, A., Obejero-Paz, C. A., Konieczkowski, M., Sedor, J. R., and Schelling, J. R. (2004) *J. Biol. Chem.* **279**, 26280–26286
- Baumgartner, M., Patel, H., and Barber, D. L. (2004) *Am. J. Physiol. Cell Physiol.* **287**, C844–C850
- Hilgemann, D. W., and Ball, R. (1996) *Science* **273**, 956–959
- Rohács, T., Lopes, C. M., Jin, T., Ramdya, P. P., Molnár, Z., and Logothetis, D. E. (2003) *Proc. Natl. Acad. Sci. U.S.A.* **100**, 745–750
- Pochynuk, O., Tong, Q., Staruschenko, A., Ma, H. P., and Stockand, J. D. (2006) *Am. J. Physiol. Renal Physiol.* **290**, F949–F957

27. Rohacs, T. (2009) *Cell Calcium* **45**, 554–565
28. Mohan, S., Tse, C. M., Gabelli, S. B., Sarker, R., Cha, B., Fahie, K., Nadella, M., Zachos, N. C., Tu-Sekine, B., Raben, D., Amzel, L. M., and Donowitz, M. (2010) *J. Biol. Chem.* **285**, 34566–34578
29. Aharonovitz, O., Zaun, H. C., Balla, T., York, J. D., Orłowski, J., and Grinstein, S. (2000) *J. Cell Biol.* **150**, 213–224
30. Fuster, D., Moe, O. W., and Hilgemann, D. W. (2004) *Proc. Natl. Acad. Sci. U.S.A.* **101**, 10482–10487
31. Wakabayashi, S., Nakamura, T. Y., Kobayashi, S., and Hisamitsu, T. (2010) *J. Biol. Chem.* **285**, 26652–26661
32. Bullis, B. L., Li, X., Singh, D. N., Berthiaume, L. G., and Fliegel, L. (2002) *Eur. J. Biochem.* **269**, 4887–4895
33. Bourguignon, L. Y., Singleton, P. A., Diedrich, F., Stern, R., and Gilad, E. (2004) *J. Biol. Chem.* **279**, 26991–27007
34. Fujita, A., Cheng, J., Tauchi-Sato, K., Takenawa, T., and Fujimoto, T. (2009) *Proc. Natl. Acad. Sci. U.S.A.* **106**, 9256–9261
35. Gamper, N., and Shapiro, M. S. (2007) *Nat. Rev. Neurosci.* **8**, 921–934
36. McLaughlin, S., Wang, J., Gambhir, A., and Murray, D. (2002) *Annu. Rev. Biophys. Biomol. Struct.* **31**, 151–175
37. Liu, A. P., and Fletcher, D. A. (2006) *Biophys. J.* **91**, 4064–4070
38. Blin, G., Margeat, E., Carvalho, K., Royer, C. A., Roy, C., and Picart, C. (2008) *Biophys. J.* **94**, 1021–1033
39. Mejillano, M., Yamamoto, M., Rozelle, A. L., Sun, H. Q., Wang, X., and Yin, H. L. (2001) *J. Biol. Chem.* **276**, 1865–1872
40. Wu, Y., Tibrewal, N., and Birge, R. B. (2006) *Trends Cell Biol.* **16**, 189–197
41. Lagana, A., Vadnais, J., Le, P. U., Nguyen, T. N., Laprade, R., Nabi, I. R., and Noël, J. (2000) *J. Cell Sci.* **113**, 3649–3662
42. Cox, G. A., Lutz, C. M., Yang, C. L., Biemesderfer, D., Bronson, R. T., Fu, A., Aronson, P. S., Noebels, J. L., and Frankel, W. N. (1997) *Cell* **91**, 139–148
43. Schelling, J. R., Hanson, A. S., Marzec, R., and Linas, S. L. (1992) *J. Clin. Invest.* **90**, 2472–2480
44. Orłowski, J., Kandasamy, R. A., and Shull, G. E. (1992) *J. Biol. Chem.* **267**, 9331–9339
45. Wu, K. L., Khan, S., Lakhe-Reddy, S., Wang, L., Jarad, G., Miller, R. T., Konieczkowski, M., Brown, A. M., Sedor, J. R., and Schelling, J. R. (2003) *Am. J. Physiol. Renal Physiol.* **284**, F829–F839
46. Lishko, V. K., Podolnikova, N. P., Yakubenko, V. P., Yakovlev, S., Medved, L., Yadav, S. P., and Ugarova, T. P. (2004) *J. Biol. Chem.* **279**, 44897–44906
47. Schelling, J. R., DeLuca, D. J., Konieczkowski, M., Marzec, R., Sedor, J. R., Dubyak, G. R., and Linas, S. L. (1994) *Kidney Int.* **46**, 675–682
48. Naga Prasad, S. V., Jayatilleke, A., Madamanchi, A., and Rockman, H. A. (2005) *Nat. Cell Biol.* **7**, 785–796
49. Cooke, F. T. (2010) *Methods Mol. Biol.* **645**, 179–202
50. Gassama-Diagne, A., Yu, W., ter Beest, M., Martin-Belmonte, F., Kierbel, A., Engel, J., and Mostov, K. (2006) *Nat. Cell Biol.* **8**, 963–970
51. Martin-Belmonte, F., Gassama, A., Datta, A., Yu, W., Rescher, U., Gerke, V., and Mostov, K. (2007) *Cell* **128**, 383–397
52. Shinlapawattayatorn, K., Dudash, L. A., Du, X. X., Heller, L., Poelzing, S., Ficker, E., and Deschenes, I. (2011) *Circ. Cardiovasc. Genet.*, in press
53. Bal, M., Zaika, O., Martin, P., and Shapiro, M. S. (2008) *J. Physiol.* **586**, 2307–2320
54. Lacowicz, J. R. (2006) in *Principles of Fluorescence Spectroscopy* (Lacowicz, J. R., ed) 3rd Ed., Chapter 13, pp. 443–475, Springer, New York
55. Bachmann, O., Franke, K., Yu, H., Riederer, B., Li, H. C., Soleimani, M., Manns, M. P., and Seidler, U. (2008) *BMC Cell Biol.* **9**, 70
56. Di Paolo, G., and De Camilli, P. (2006) *Nature* **443**, 651–657
57. Várnai, P., Bondeva, T., Tamás, P., Tóth, B., Buday, L., Hunyady, L., and Balla, T. (2005) *J. Cell Sci.* **118**, 4879–4888
58. Khan, S., Wu, K. L., Sedor, J. R., Abu Jawdeh, B. G., and Schelling, J. R. (2006) *Cell Mol. Biol.* **52**, 115–121
59. Lindsay, Y., McCoull, D., Davidson, L., Leslie, N. R., Fairservice, A., Gray, A., Lucocq, J., and Downes, C. P. (2006) *J. Cell Sci.* **119**, 5160–5168
60. Miao, B., Skidan, I., Yang, J., Lugovskoy, A., Reibarkh, M., Long, K., Brazell, T., Durugkar, K. A., Maki, J., Ramana, C. V., Schaffhausen, B., Wagner, G., Torchilin, V., Yuan, J., and Degterev, A. (2010) *Proc. Natl. Acad. Sci. U.S.A.*
61. Wang, J., Arbuzova, A., Hangyás-Mihályiné, G., and McLaughlin, S. (2001) *J. Biol. Chem.* **276**, 5012–5019
62. Papayannopoulos, V., Co, C., Prehoda, K. E., Snapper, S., Taunton, J., and Lim, W. A. (2005) *Mol. Cell* **17**, 181–191
63. Cheng, W. W., D'Avanzo, N., Doyle, D. A., and Nichols, C. G. (2011) *Biophys. J.* **100**, 620–628
64. Hansen, S. B., Tao, X., and MacKinnon, R. (2011) *Nature* **477**, 495–498
65. Denker, S. P., Huang, D. C., Orłowski, J., Furthmayr, H., and Barber, D. L. (2000) *Mol. Cell* **6**, 1425–1436
66. Frantz, C., Barreiro, G., Dominguez, L., Chen, X., Eddy, R., Condeelis, J., Kelly, M. J., Jacobson, M. P., and Barber, D. L. (2008) *J. Cell Biol.* **183**, 865–879
67. Dibrov, P., Murtazina, R., Kinsella, J., and Fliegel, L. (2000) *Biosci. Rep.* **20**, 185–197
68. Huang, B. X., Akbar, M., Kevala, K., and Kim, H. Y. (2011) *J. Cell Biol.* **192**, 979–992
69. Alexander, R. T., Jaumouillé, V., Yeung, T., Furuya, W., Peltekova, I., Boucher, A., Zasloff, M., Orłowski, J., and Grinstein, S. (2011) *EMBO J.* **30**, 679–691
70. Orłowski, J. (1993) *J. Biol. Chem.* **268**, 16369–16377
71. Kapus, A., Grinstein, S., Wasan, S., Kandasamy, R., and Orłowski, J. (1994) *J. Biol. Chem.* **269**, 23544–23552
72. Nath, S. K., Hang, C. Y., Levine, S. A., Yun, C. H., Montrose, M. H., Donowitz, M., and Tse, C. M. (1996) *Am. J. Physiol.* **270**, G431–G441
73. Soleimani, M., Watts, B. A., 3rd, Singh, G., and Good, D. W. (1998) *Kidney Int.* **53**, 423–431
74. Snabaitis, A. K., Cuello, F., and Avkiran, M. (2008) *Circ. Res.* **103**, 881–890
75. Meima, M. E., Webb, B. A., Witkowska, H. E., and Barber, D. L. (2009) *J. Biol. Chem.* **284**, 26666–26675
76. Kunkel, M. T., Ni, Q., Tsien, R. Y., Zhang, J., and Newton, A. C. (2005) *J. Biol. Chem.* **280**, 5581–5587